JACS
JOURNAL OF THE AMERICAN CHEMICAL SOCIETY
Communication
pubs.acs.org/JACS

Order–Disorder Transition of Dipolar Rotor in a Crystalline Molecular Gyrotop and Its Optical Change

Wataru Setaka*,† and Kentaro Yamaguchi‡

†Division of Applied Chemistry, Urban Environmental Sciences, Tokyo Metropolitan University, Hachioji, Tokyo 192-0397, Japan
‡Pharmaceutical Sciences at Kagawa Campus, Tokushima Bunri University, Sanuki, Kagawa 769-2193, Japan

Supporting Information

ABSTRACT: Successful control of the orientation of the π-electron systems in media has been achieved in certain liquid crystals, making them applicable to devices for optical systems because of the variation in the optical properties with the orientation of the π-electron system. However, because of close packing, changing the orientation of molecules in the crystalline state is usually difficult. A macrocage molecule with a bridged thiophene rotor was synthesized as a molecular gyrotop having a dipolar rotor, given that the dipole derived from the thiophene can rotate even in the crystal. The thermally induced change in the orientation of the dipolar rotors (thiophene ring) inside the crystal, i.e., order–disorder transition, and the variation in the optical properties in the crystalline state were observed.

The chemistry and properties of molecular machines, in which mechanical motions of parts of the molecules are observed, have been extensively studied.[1−9] Macrocage molecules with a bridged rotor have been synthesized as molecular gyroscopes and molecular gyrotops given that the rotor can rotate even in the crystalline state.[2−8] Recently, we reported thermal modulation of the birefringence of a molecular gyrotop crystal possessing a phenylene rotor encased in three long alkyl-spokes as the first application of variation in the optical properties because of the dynamics of the phenylene rotor in a crystal.[8]

Molecular gyroscopes or gyrotops with a dipolar rotor, sometimes referred to as molecular compasses, have also been reported.[7] Study of the orientation of rotating dipoles is of interest in terms of the physics of nanoscale materials. Clarke, Garcia-Garibay, et al. recently characterized the rotational dynamics of rotor–rotor interactions within crystalline three-dimensional arrays of dipolar molecular rotors.[7] Akutagawa et al. have also reported supramolecular rotors of $[Ni(dmit)_2]^-$ salts ($dmit_2^-$ = 2-thioxo-1,3-dithiole-4,5-dithiolate) exhibiting ferroelectric properties.[10] Study of the orientation and dipole–dipole interactions in arrays of dipolar molecular rotors remains important to understanding the dielectric properties of materials and the dynamics of the dipolar rotors. We demonstrate the order–disorder transition of the orientation of the dipolar rotor in a molecular gyrotop using X-ray crystallographic analysis and solid-state NMR spectroscopy and variation in the optical properties in the crystalline state.

The molecular design for this experiment is as follows: a molecular gyrotop consists of a frame cage and a rotor (Figure 1). Derivatives of our previous molecular gyrotop having a phenylene rotor encased in three tetradecyl-spokes were first synthesized. In order to introduce a dipole into the rotor, a thiophene ring with a dipole moment of 0.52 D[11] was applied as a rotor. The position of the thiophene ring can be easily determined by X-ray diffraction study because of the presence of the sulfur atom. The tetradecyl-spokes are utilized for the cage, given that the size of the thiophene rotor is comparable to the phenylene rotor.

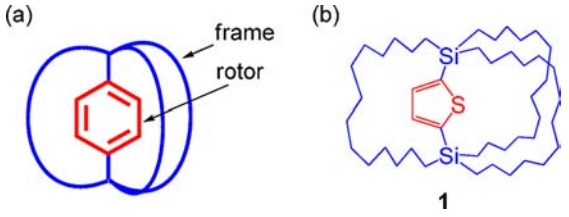

Figure 1. (a) Schematic representation of a molecular gyrotop, i.e., consists of a frame cage and a rotor, and (b) structural formula of the molecular gyrotop **1**.

Synthesis of the molecular gyrotop having a thiophene rotor **1** was achieved as shown in Scheme 1.[12] The cage compound **1** was synthesized by ring closing metathesis of 1,4-bis(tri-7-octenyl)silylthiophene **2**, which was synthesized by reaction of dilithiothiophene with a corresponding trialkenylchlorosilane,

Scheme 1. Synthesis of Molecular Gyrotop 1

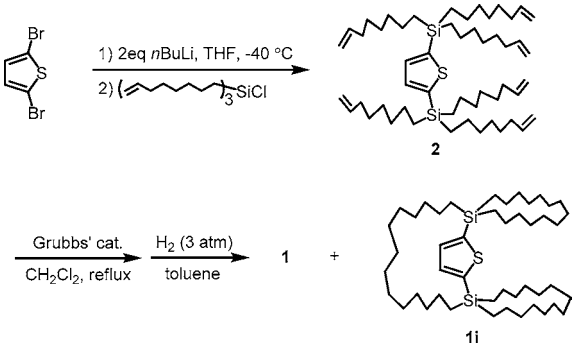

Received: August 16, 2013
Published: September 18, 2013

dx.doi.org/10.1021/ja408405f | J. Am. Chem. Soc. 2013, 135, 14560−14563

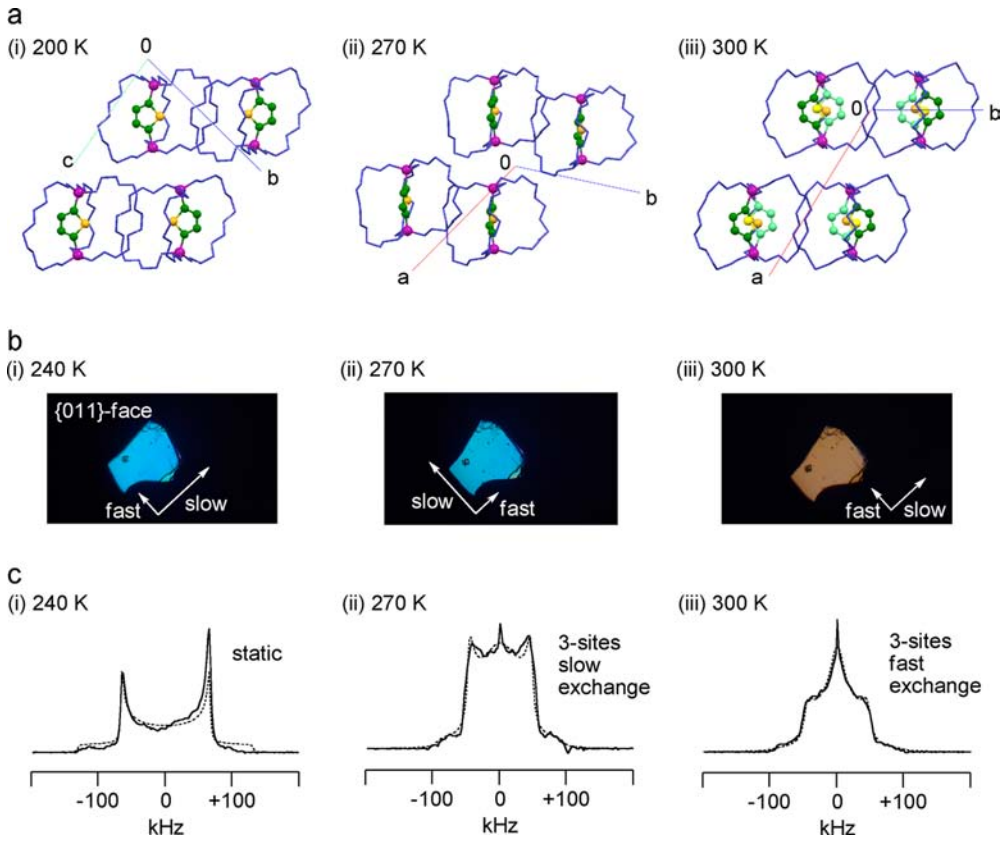

Figure 2. (a) Temperature dependence of crystal structures of **1** determined via X-ray crystallography. (b) Photographs of the single crystals of **1** upon irradiation with polarized white light (the light passed through the crystal along the rotational axes of the molecules, i.e., through the ⟨011⟩ axis, at 200 K) [Directions of two optical axes (fast and slow axes) are shown. For details, see Figure S20.] (c) Temperature-dependent solid-state ^{2}H NMR spectra of **1**-d_2 [solid line: observed spectra; dotted line: spectra simulated spectra. For details, see Figure S15].

with subsequent hydrogenation under hydrogen pressure of 3 atm using Pd/C as a catalyst. Preparative recycling GPC was used to isolate the desired cages from the reaction mixture, which also contained the structural isomer **1i** and polymeric byproducts. The ratio of formation of **1** to **1i** was 10:1. The structures of **1** and **1i** were confirmed via ^{1}H, ^{13}C, and ^{29}Si NMR spectroscopy. The ^{1}H and ^{13}C NMR spectra of **1** demonstrated that, in solution, the three alkyl-chains were identical, indicating that the thiophene ring rotates rapidly inside the cage.

Recrystallization of **1** from a mixture of tetrahydrofuran and methanol afforded a single crystal; unfortunately, isomer **1i** was not crystallized. Figure 2a(i) shows the structure of **1** in the single crystal at 200 K (CP-I).[13] In the crystals, the molecules were arranged by their rotation axes. Because the thiophene ring has a dipole moment, the direction of the ring inside the crystal is also important for analysis of the intermolecular dipole−dipole interactions. The rings were oriented diametrically opposite to each other to cancel out polarization of the crystal at 200 K. Interestingly, the orientation and direction of the thiophene ring inside the crystal were temperature-dependent, and three crystal phases could be observed by temperature-dependent X-ray crystallographic analysis of **1** at 200 K (CP-I), 270 K (CP-II), and 300 K (CP-III). The direction of the thiophene ring of **1** in the CP-II crystal is perpendicular to the structure in both CP-I and CP-III, and the rings were oriented completely opposite one to another to cancel out the polarization of the crystal as shown in Figure 2a(ii). In other words, the alignment of the ring was ordered, but the direction of the entire ring was perpendicular to that of CP-I. Figure 2a(iii) shows the crystal structure of CP-III of **1**. The overall position of the ring is similar to that of CP-I, which is perpendicular to CP-II. The thiophene ring was observed at two sites with occupancy factors of 0.5, respectively. These results indicate that the rings orient randomly between the two sites with exchange, and the average population of the sites is 1:1. Therefore, order−disorder transition of the orientation of the dipolar rotor in the crystal was observed between CP-I/CP-II and CP-III.

In accordance with the orientational change of the dipolar rotor in the crystal induced by varying the temperature, changes in the optical properties of the crystal were also apparent.[8,14] The birefringence (Δn), which is the difference between the two refraction indices (of the slow and fast optical axes), can be analyzed by measuring the interference colors due to retardation upon irradiation of the crystal with polarized white light.[15] A photograph of a single crystal of **1** is shown in Figure 2b. The widest face of the crystal corresponds to the {011}-face as determined by X-ray diffraction at 200 K. By viewing this crystal face, molecular aggregation is observed along the rotational axis. Figure 2b also shows photographs of the single crystal of **1** (the {011}-face at 200 K (CP-I)) upon irradiation with polarized white light at various temperatures. Interference colors (blue at 200 K) due to retardation were observed. The colors remained unchanged during the course of the transition from CP-I to CP-II. At 285 K, the interference color changed discontinuously from blue to yellow because of the phase transition from CP-II to CP-III. Notably, the

dx.doi.org/10.1021/ja408405f | J. Am. Chem. Soc. 2013, 135, 14560−14563

directions of the fast and slow optical axes of the crystal were exchanged among CP-I, -III, and -II as depicted in the figure. This observation is closely related to the fact that the overall position of the thiophene ring inside the crystal of CP-II was perpendicular to that of CP-I,-III. Therefore, this is direct evidence that the refractive indices of the crystal depended primarily on the orientation of the thiophene. In addition, during the phase transitions, the external morphology of the crystal was also slightly changed.

Figure 3 shows a plot of the temperature dependence of Δn, derived from the observed retardation divided by the crystal

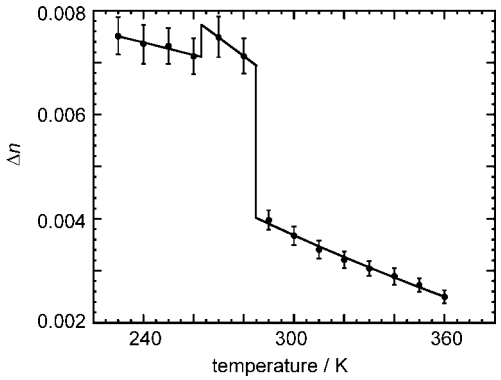

Figure 3. Plot of Δn versus temperature for the crystal of **1** on the crystal face ({011}-face at 200 K).

thickness (i.e., optical path length).[15] The value of Δn is apparently large at low temperature. With increasing temperature, Δn decreased slightly, with a discontinuous change because of the phase transition from CP-I to CP-II at 263 K. At 285 K, Δn decreased discontinuously because of the phase transition from CP-II to CP-III. Thus, the birefringence (Δn) of the crystal face is relatively large below 285 K because of the ordered orientation of the thiophene in the crystal. Above 285 K, Δn decreased because of the disordered orientation of the thiophene in the crystal. These structural and optical property changes are completely reversible, at least in the temperature range from 230 to 370 K. These results indicate that the birefringence of the crystal was completely different for the ordered and disordered orientations of the thiophene ring.

Dynamic motions of the thiophene rotor in the crystal were estimated using solid-state NMR spectroscopy.[16] Detailed temperature-dependent quadrupolar echo ^{2}H NMR spectra of **1**-d_2, in which the thiophene moiety was labeled with two deuterium atoms, acquired at 10 K intervals in the temperature range of 240−350 K, are shown in Figure S15. Figure 2c shows representative ^{2}H NMR spectra observed at each crystal phase. For CP-I (240 K), the thiophene ring was static. In the case of CP-II (270 K), the thiophene ring underwent slow site exchange among the three equilibrium sites, which are located every 120° around an axis of rotation. The occupancy factors for each site and the rates of flipping were estimated by simulation of the spectral line shapes (Pake pattern).[17] In the case of CP-III (280 K), rapid three-site exchange of the thiophene rotor was observed. Although the thiophene positions were disordered in CP-III based on X-ray structural analysis, inversion of the ring was not observed in ^{2}H NMR analysis, plausibly because of the very low frequency of the inversion. Nevertheless, these results indicate that the dynamic modes of the thiophene were switched during phase transition of the crystal and that the motion of the thiophene became vigorous with increasing temperature.

The temperature dependence of the crystal phase transformation can be explained by assuming that the molar Gibbs free energies (ΔG), i.e., chemical potentials (μ), of the crystal phases depend primarily on that of the molecule, although the present analysis is quite qualitative. Figure 4 shows a schematic

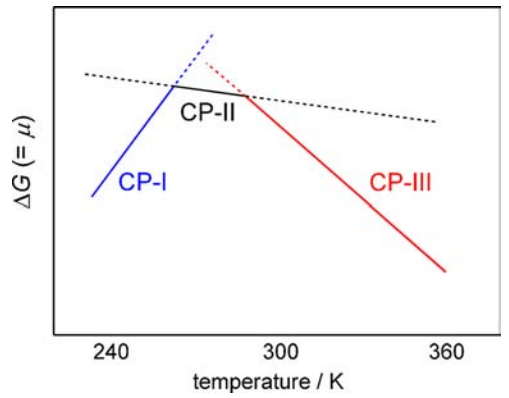

Figure 4. Schematic Gibbs free energy vs temperature diagram for the multiphases of the molecular gyrotop **1**.

molar Gibbs free energy (ΔG) versus temperature (T) diagram for the multiphases of the molecular gyrotop **1**. The y-intercept and the slope of the graph indicate ΔH and $-\Delta S$, respectively ($\Delta G = \Delta H - T\Delta S$). ΔH depends on the stability of the molecule, especially the cage structure. The cage structure of CP-I is the most stable among the phases given that the static thiophene ring is wrapped by the folded cage, based on theoretical calculation (Supporting Information Figure S21). Thus, the molecular structure of CP-I has the lowest ΔH value among the crystal phases. On the other hand, rotation of the thiophene in CP-I was prohibited, indicative of the negative ΔS in CP-I. The thiophene in CP-III can be oriented in several directions during the dynamic motion, indicating the large ΔS in CP-III. The solid lines shown in the graph indicate the stable phases, i.e., those with the lowest chemical potential at each temperature. It is thus concluded that these crystal phase transitions were induced by switching between the static and the dynamic modes of the rotor within the crystal.

In summary, the temperature-dependent order−disorder transition of the orientation of a dipolar rotor was experimentally observed in the crystal state for the molecular gyrotop **1** having a thiophene rotor. The ordering of the alignment of the dipolar rotor may be ascribed to intermolecular dipole−dipole interactions. The orientation of the dipolar rotors becomes disordered above the transition temperature given that the thermal noise (kT) is sufficiently large relative to the stabilization energy for alignment of the dipoles and the rotational energy barrier. The optical properties, such as the refractive indices, of the crystal were primarily dependent on the orientation of the thiophene. Thus, single crystals of these molecular gyrotops with a dipolar rotor may be applicable to devices for optical systems, and orientational changes of the dipolar rotor in the crystal can easily be detected by observation using a polarized-light microscope.

dx.doi.org/10.1021/ja408405f | J. Am. Chem. Soc. 2013, 135, 14560−14563

■ ASSOCIATED CONTENT

Supporting Information

Experimental details and characterization data. This material is available free of charge via the Internet at http://pubs.acs.org.

■ AUTHOR INFORMATION

Corresponding Author

wsetaka@tmu.ac.jp

Notes

The authors declare no competing financial interest.

■ ACKNOWLEDGMENTS

This work was supported by a JSPS Grant-in-Aid for Scientific Research (B) (no. 25288042) and the Nagase Science and Technology Foundation (W.S.).

■ REFERENCES

(1) (a) Vogelsberg, C. S.; Garcia-Garibay, M. A. *Chem. Soc. Rev.* **2012**, *41*, 1892. (b) Karim, A. R.; Linden, A.; Baldridge, K. K.; Siegel, J. S. *Chem. Sci.* **2010**, *1*, 102. (c) Blanzani, V.; Credi, A.; Venturi, M. *Molecular Devices and Machines*, 2nd ed.; Wiley-VCH: Weinheim, 2008. (d) Leigh, D. A.; Zerbetto, F.; Kay, E. R. *Angew. Chem., Int. Ed.* **2007**, *46*, 72. (e) Browne, W. R.; Feringa, B. L. *Nat. Nanotechnol.* **2006**, *1*, 25. (f) Kelly, T. R. *Molecular Machines. Topics in Current Chemistry*; Springer: Hidelberg, 2005; Vol. *262*. (g) Kottas, G. S.; Clarke, L. I.; Horinek, D.; Michl, J. *Chem. Rev.* **2005**, *105*, 1281. (h) Garcia-Garibay, M. A. *Proc. Natl. Acad. Sci. U.S.A.* **2005**, *102*, 10771. (i) Blanzani, V.; Credi, A.; Raymo, R.; Stoddart, J. F. *Angew. Chem., Int. Ed.* **2000**, *39*, 3348.

(2) (a) Dominguez, Z.; Dang, H.; Strouse, M. J.; Garcia-Garibay, M. A. *J. Am. Chem. Soc.* **2002**, *124*, 2398. (b) Godinez, C. E.; Zepeda, G.; Garcia-Garibay, M. A. *J. Am. Chem. Soc.* **2002**, *124*, 4701. (c) Dominguez, Z.; Dang, H.; Strouse, J. M.; Garcia-Garibay, M. A. *J. Am. Chem. Soc.* **2002**, *124*, 7719. (d) Dominguez, Z.; Khuong, T. A. V.; Sanrame, C. N.; Dang, H.; Nuñez, J. E.; Garcia-Garibay, M. A. *J. Am. Chem. Soc.* **2003**, *125*, 8827.

(3) (a) Rodríguez-Molina, B.; Pérez-Estrada, S.; Garcia-Garibay, M. A. *J. Am. Chem. Soc.* **2013**, *135*, 10388. (b) Czajkowska-Szczykowska, D.; Rodríguez-Molina, B.; Magaña-Vergara, N. E.; Santillan, R.; Morzycki, J. W.; Garcia-Garibay, M. A. *J. Org. Chem.* **2012**, *77*, 9970. (c) Commins, P.; Nuñez, J. E.; Garcia-Garibay, M. A. *J. Org. Chem.* **2011**, *76*, 8355. (d) Commins, P.; Nuñez, J. E.; Garcia-Garibay, M. A. *J. Org. Chem.* **2011**, *76*, 8355. (e) Nuñez, J. E.; Natarajan, A.; Khan, S. I.; Garcia-Garibay, M. A. *Org. Lett.* **2007**, *9*, 3559.

(4) (a) Zeits, P. D.; Rachiero, G. P.; Hampel, F.; Reibenspies, J. H.; Gladysz, J. A. *Organometallics* **2012**, *31*, 2854. (b) Skopek, K.; Gladysz, J. A. *J. Organomet. Chem.* **2008**, *693*, 857. (c) Skopek, K.; Barbasiewicz, M.; Hampel, F.; Gladysz, J. A. *Inorg. Chem.* **2008**, *47*, 3474. (d) Han, J.; Deng, C.; Wang, L.; Gladysz, J. A. *Organometallics* **2010**, *29*, 3231. (e) Heß, G. D.; Hampel, F.; Gladysz, J. A. *Organometallics* **2007**, *26*, 5129. (f) Wang, L.; Shima, T.; Hampel, F.; Gladysz, J. A. *Chem. Commun.* **2006**, 4075. (g) Wang, L.; Hampel, F.; Gladysz, J. A. *Angew. Chem., Int. Ed.* **2006**, *45*, 4372. (h) Narwara, A. J.; Shima, T.; Hampel, F.; Gladysz, J. A. *J. Am. Chem. Soc.* **2006**, *128*, 4962. (i) Shima, T.; Hampel, F.; Gladysz, J. A. *Angew. Chem., Int. Ed.* **2004**, *43*, 5537.

(5) (a) Marahatta, A. B.; Kanno, M.; Hoki, K.; Setaka, W.; Irle, S.; Kono, H. *J. Phys. Chem. C* **2012**, *116*, 24845. (b) Setaka, W.; Ohmizu, S.; Kira, M. *Chem. Lett.* **2010**, *39*, 468. (c) Setaka, W.; Ohmizu, S.; Kabuto, C.; Kira, M. *Chem. Lett.* **2007**, *36*, 1076.

(6) (a) Khan, N. S.; Perez-Aguilar, J. M.; Kaufmann, T.; Hill, P. A.; Taratula, O.; Lee, O.-S.; Carroll, P. J.; Saven, J. G.; Dmochowski, I. J. *J. Org. Chem.* **2011**, *76*, 1418. (b) Kitagawa, H.; Kobori, Y.; Yamanaka, M.; Yoza, K.; Kobayashi, K. *Proc. Natl. Acad. Sci. U.S.A.* **2009**, *106*, 10444. (c) Sugino, H.; Kawai, H.; Fujiwara, K.; Suzuki, T. *Chem. Lett.* **2012**, *41*, 79. (d) Shustova, N. B.; Ong, T.-C.; Cozzolino, A. F.; Michaelis, V. K.; Griffin, R. G.; Dincă, M. *J. Am. Chem. Soc.* **2012**, *134*, 15061. (e) Vogelsberg, C. S.; Bracco, S.; Beretta, M.; Comotti, A.; Sozzani, P.; Garcia-Garibay, M. A. *J. Phys. Chem. B* **2012**, *116*, 1623. (f) Comotti, A.; Bracco, S.; Valsesia, P.; Beretta, M.; Sozzani, P. *Angew. Chem., Int. Ed.* **2010**, *49*, 1760. (g) Brustolon, M.; Barbon, A.; Bortolus, M.; Maniero, A. L.; Sozzani, P.; Comotti, A.; Simonutti, R. *J. Am. Chem. Soc.* **2004**, *126*, 15512.

(7) (a) Horansky, R. D.; Clarke, L. I.; Winston, E. B.; Price, J. C.; Karlen, S. D.; Jarowski, P. D.; Santillan, R.; Garcia-Garibay, M. A. *Phys. Rev. B* **2006**, *74*, 054306. (b) Horansky, R. D.; Clarke, L. I.; Price, J. C.; Khuong, T.-A. V.; Jarowski, P. D.; Garcia-Garibay, M. A. *Phys. Rev. B* **2005**, *72*, 014302. (c) Dominguez, Z.; Khuong, T.-A. V.; Dang, H.; Sanrame, C. N.; Nuñez, J. E.; Garcia-Garibay, M. A. *J. Am. Chem. Soc.* **2003**, *125*, 8827.

(8) (a) Setaka, W.; Yamaguchi, K. *Proc. Natl. Acad. Sci. U.S.A.* **2012**, *109*, 9260. (b) Setaka, W.; Yamaguchi, K. *J. Am. Chem. Soc.* **2012**, *134*, 12458. (c) Setaka, W.; Koyama, A.; Yamaguchi, K. *Org. Lett.* **2013**, DOI: 10.1021/ol402464d.

(9) Lemouchi, C.; Iliopoulos, K.; Zorina, L.; Simonov, S.; Wzietek, P.; Cauchy, T.; Rodríguez-Fortea, A.; Canadell, E.; Kaleta, J.; Michl, J.; Gindre, D.; Chrysos, M.; Batail, P. *J. Am. Chem. Soc.* **2013**, *135*, 9366.

(10) Akutagawa, T.; Koshinaka, H.; Sato, D.; Takeda, S.; Noro, S.; Takahashi, H.; Kumai, R.; Tokura, Y.; Nakamura, T. *Nat. Mater.* **2005**, *8*, 342.

(11) Barton, T. J.; Roth, R. W.; Verkade, J. G. *J. Am. Chem. Soc.* **1972**, *94*, 8854.

(12) For details, see SI.

(13) Diffraction data of **1** were collected on a Bruker APEX-II CCD system using graphite-monochromatized MoKα radiation (λ = 0.71069 Å). Crystal data at 200 K, triclinic, P-1, a = 11.801(6) Å, b = 14.19(1) Å, c = 16.457(9) Å, α = 75.294(9)°, β = 75.221(6)°, γ = 66.078(6)°, V = 2400(2) Å^3, R_1 = 0.0742 ($I > 2\sigma I$), wR_2 = 0.2400 (all data). Crystallographic data were deposited in the Cambridge Crystallographic Database Centre (CCDC-951777). Details for the X-ray structural analyses of **1** at 300 and 340 K were shown in SI.

(14) (a) Horie, M.; Suzaki, Y.; Hashizume, D.; Abe, T.; Wu, T.; Sassa, T.; Hosokai, T.; Osakada, K. *J. Am. Chem. Soc.* **2012**, *134*, 17932. (b) Horie, M.; Sassa, T.; Hashizume, D.; Suzaki, Y.; Osakada, K.; Wada, T. *Angew. Chem., Int. Ed.* **2007**, *46*, 4983.

(15) Fast and slow optical axes were confirmed using a polarized-light microscope (Olympus BX51) equipped with a sensitive color plate. Retardations were observed by a polarized-light microscope (Olympus BX51) equipped with a Berek compensator and monochromatic light at 546 nm generated using a color filter. The Δn was calculated from retardation/thickness. The thickness of the crystal was measured to be 98.7 ± 1.5 μm using a laser displacement sensor (KEYENCE LT-9010M) at 300 K. Further details are given in SI.

(16) Temperature-dependent solid-state ^{2}H NMR spectra were recorded on Varian Unity 500 spectrometers, using a quadrupolar echo pulse sequence (d_1-90° pulse-τ_1-90° pulse-τ_2-FID; 90° pulse = 3.95 μs, τ_1 = 30 μs, τ_2 = 20 μs, d_1 = 3−5 s). Simulations of ^{2}H NMR spectra were carried out on NMR-WEBLAB. Further details are given in SI.

(17) Macho, V.; Brombacher, L.; Spiess, H. W. *Appl. Magn. Reson.* **2001**, *20*, 405.